Flood Impact Pressure Analysis of Vertical Wall Structures using PLIC-VOF Method with Lagrangian Advection Algorithm

Phan, Hoang-Nam* Lee, Jee-Ho†

Abstract

The flood impact pressure acting on a vertical wall resulting from a dam-breaking problem is simulated using a navier-Stokes(N-S) solver. The N-S solver uses Eulerian Finite Volume Method(FVM) along with Volume Of Fluid(VOF) method for 2-D incompressible free surface flows. A Split Lagrangian Advection(SLA) scheme for VOF method is implemented in this paper. The SLA scheme is developed based on an algorithm of Piecewise Linear Interface Calculation(PLIC). The coupling between the continuity and momentum equations is affected by using a well-known Semi-Implicit Method for Pressure-Linked Equations (SIMPLE) algorithm. Several two-dimensional numerical simulations of the dam-breaking problem are presented to validate the accuracy and demonstrate the capability of the present algorithm. The significance of the time step and grid resolution are also discussed. The computational results are compared with experimental data and with computations by other numerical methods. The results showed a favorable agreement of water impact pressure as well as the global fluid motion.

Keywords : *flood impact pressure, dam break, finite volume method, volume of fluid method, lagrangian advection, simple algorithm*

1. Introduction

Recently, theoretical and experimental studies show the necessity of dynamic analysis, including hydrodynamic pressure of the free surface flows in design and safety assessment of dam structures. Therefore, development of reliable analysis tools which can precisely predict the water impact pressure load acting on the upstream face of a dam structure, is crucial.

The numerical models developed for prediction of water impact pressure are mainly based on Navier-Stokes equations, which describe the motion of fluid flows. Most solution methods for the unsteady incompressible Navier-Stokes equations use the fixed grid approach and they should be coupled with mathematical treatment of the free surface. Surface-capturing or volume tracking methods are known as the numerical techniques which have a potential of dealing with large free surface deformation on the fixed grid.

One of the earliest volume tracking methods for material interfaces is the Marker And Cell (MAC) method introduced by Harlow and Welch (1965). In this method, marker particles are inserted to identify the spatial region occupied by a single fluid with a free surface. The most popular capturing method for advecting interfaces is the Volume Of Fuid (VOF) method, which defines the interface by calculating the fractional volume of each material occupied in each computational cell. Two early approaches are the Simple Line Interface Calculation (SLIC) algorithm (Noh and Woodward, 1976) and the VOF algorithm (Hirt and Nichols, 1981), in which the interface is represented as a piecewise-constant line in each

† 책임저자, 정회원 · 동국대학교-서울 토목환경공학과 교수
Tel: 02-2260-3352 ; Fax: 02-2266-8753
E-mail: jeeholee@dgu.edu
* 동국대학교-서울 토목환경공학과 석사과정

• 이 논문에 대한 토론을 2011년 2월 28일까지 본 학회에 보내주시면 2011년 4월호에 그 결과를 게재하겠습니다.

interfacial cell, either vertically or horizontally. Later developments include the Piecewise Linear Interface Calculation (PLIC) proposed by Youngs (1986) and further developed by other researchers (Kothe and Rider, 1998; Zaleski *et al.*, 2003; Veldman *et al.*, 2005). The PLIC method approximates the interface by a straight line of arbitrary orientation in each cell. Its orientation is determined the distribution of one of the fluids in the neighbor cell.

The advection schemes in the VOF method fall into two categories: the operator split method and the unsplit method. In the present study, the operator split scheme, where boundary fluxes at each time step are calculated independently, is used. The explicit Lagrangian scheme (Li, 1995; Zaleski *et al.*, 1999; Wei *et al.*, 2010) is implemented to describe the propagation of the interface by the flow in the context of the finite volume method. The whole computational domain is subdivided into a finite number of non overlapping control volumes based on a staggered grid system. The pressure- velocity linkage is resolved by adopting an iterative solution strategy of the SIMPLE algorithm introduced by Patankar and Spalding (1972).

In this paper, a new algorithm which can combine an explicit time integration of the volume fraction equation and implicit time integration of momentum equations, is proposed. The main advantage of this coupling is the reduction of computational time in comparison with the full implicit approaches.

In Section 2, the governing equations are described. A two-dimensional PLIC-VOF method with the Lagrangian advection and a solution method for incompressible Navier-Stokes equations are discussed in Section 3. And then, the numerical simulation result of dam-breaking problems is given to show the validation and performance of the present algorithm.

2. Governing Equations

The equations governing the motion of unsteady, viscous, incompressible, immiscible two-fluid systems are the Navier-Stokes equations. In conservative form these are:

$$\frac{\partial}{\partial t}(\rho \mathbf{v}) + \nabla \cdot (\rho \mathbf{v}\mathbf{v}) = -\nabla p + \nabla \cdot \left[\mu\left(\nabla \mathbf{v} + \nabla \mathbf{v}^T\right)\right] + \mathbf{F} \tag{1}$$

where $\mathbf{v}$ is the velocity field; ρ and μ are the discontinuous density and viscosity fields, respectively; p is the pressure; $\mathbf{F}$ is the body forces.

These are supplement by the incompressible condition:

$$\nabla \cdot \mathbf{v} = 0 \tag{2}$$

If the dependent variable (scalar or vector) is denoted by ϕ, the general transport equation is written as:

$$\frac{\partial \rho\phi}{\partial t} + \nabla \cdot (\rho \mathbf{v}\phi) = \nabla \cdot (\Gamma \nabla \phi) + S_\phi \tag{3}$$

where Γ is the diffusion coefficient; S_ϕ is a source term, generally dependant on ϕ.

In the VOF method, the motion of the interface between immiscible fluids of different density and viscosity is defined by a phase indicator-the volume fraction function C which is governed by the volume fraction equation:

$$\frac{\partial C}{\partial t} + \mathbf{v} \cdot \Delta C = 0 \tag{4}$$

The volume fraction function C is equal to 1 when the cell is full, vanishes if the cell is empty and has an intermediate value when the cell contains the interface.

The properties appearing in the momentum equations are determined by the presence of the component phase in each control volume. The average values of density and viscosity are interpolated by the following formulas:

$$\begin{aligned} \rho &= C\rho_L + (1-C)\rho_A \\ \mu &= C\mu_L + (1-C)\mu_A \end{aligned} \tag{5}$$

where the subscripts L and A indicate liquid and air phases, respectively.

3. Numerical Model for Flood Impact

3.1 PLIC-VOF Interface Tracking Algorithm

3.1.1 Interface Reconstruction Scheme

The reconstruction is based on the idea that a normal vector $\boldsymbol{m}$, together with the fraction volume C, determines a unique line interface cutting the cell. In the first part of the reconstruction, a normal direction to the interface is estimated, using the method developed by Parker and Youngs (1992). We consider 3×3 block of square cells. The normal vector $\boldsymbol{m}$ is first estimated at the four corners of the central cell (i,j), for example at the top-right corner $(i+1/2,j+1/2)$ given by:

$$m_{x_1,i+1/2,j+1/2}=\frac{1}{2\Delta x_1}\left(C_{i+1,j}-C_{i,j}+C_{i+1,j+1}-C_{i,j+1}\right)$$
$$m_{x_2,i+1/2,j+1/2}=\frac{1}{2\Delta x_2}\left(C_{i,j+1}-C_{i,j}+C_{i+1,j+1}-C_{i+1,j}\right) \quad (6)$$

The required cell centered vector is obtained by averaging the four cell-corner values:

$$m_{ij}=\frac{1}{4}\left(m_{i+1/2,j-1/2}+m_{i-1/2,j-1/2}+m_{i+1/2,j+1/2}+m_{i-1/2,j+1/2}\right) \quad (7)$$

In the second part of the reconstruction, a line interface, which divides the computational cell into two parts containing the proper area of each fluid, must be found as in Fig. 1 (Zaleski *et al.*, 1999). The most general equation for the straight line in the (ξ_1, ξ_2) plane with normal $\boldsymbol{m}$ is:

$$m_1\xi_1+m_2\xi_2=\alpha \quad (8)$$

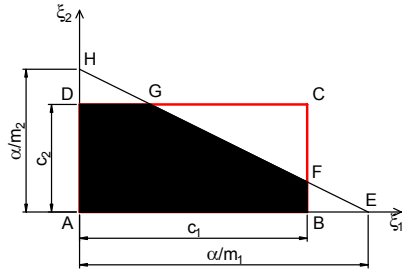

Fig. 1 The "cut" area refers to the region within the rectangular ABCD

The area of the region contained below this line within the rectangular ABCD is given by:

$$S=\frac{\alpha^2}{2m_1m_2}\left[1-H\left(\alpha-m_1c_1\right)\left(\frac{\alpha-m_1c_1}{\alpha}\right)^2-H\left(\alpha-m_2c_2\right)\left(\frac{\alpha-m_2c_2}{\alpha}\right)^2\right] \quad (9)$$

Here $H(\alpha-m_ic_i)$ is the Heaviside step function.

3.1.2 Fluid Advection Algorithm

The equation for the interface in the given cell at the initial time t_n:

$$m_1^{(n)}\xi_1^{(n)}+m_2^{(n)}\xi_2^{(n)}=\alpha^{(n)} \quad (10)$$

The velocity at any point on the free surface can be calculated through line interpolation of the velocity on cell faces, which can be expressed as:

$$v_1(\xi_1)=V_1^0\left(1-\frac{\xi_1}{c_1}\right)+V_1^{c_1}\frac{\xi_1}{c_1} \quad (11)$$

where V_1^0, V_1^{c1} are x_1-velocities on cell faces.

For each point initially ξ_1^n, the above velocity is calculated and assumed to remain constant during the advection step. Then the ξ_1^n coordinate of each point initially on the surface changes to the new value:

$$\xi_1^{(*)}=\xi_1^{(n)}+v_1\left(\xi_1^{(n)}\right)\tau=\left[1+\left(\frac{V_1^{c_1}-V_1^0}{c_1}\right)\tau\right]\xi_1^{(n)}+V_1^0\tau \quad (12)$$

$$\xi_1^{(n)}=\frac{\xi_1^{(*)}-V_1^0\tau}{1+\left(\left(V_1^{c_1}-V_1^0\right)/c_1\right)\tau} \quad (13)$$

The equation for the interface after advection:

$$m_1^{(*)}\xi_1^{(*)}+m_2^{(n)}\xi_2^{(n)}=\alpha^{(*)} \quad (14)$$

where,

$$m_1^{(*)}=\frac{m_1^{(n)}}{1+\left(\left(V_1^{c_1}-V_1^0\right)/c_1\right)\tau} \quad (15)$$

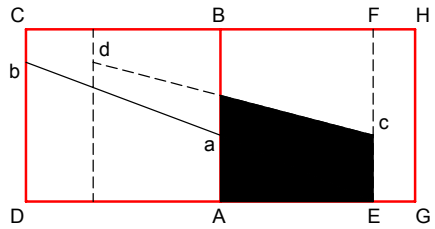

Fig. 2 A schematic illustration of the Lagrangian advection of the interface

$$\alpha^{(*)} = \alpha^{(n)} + \frac{m_1^{(n)} V_1^0 \tau}{1 + \left(\left(V_1^{c_1} - V_1^0 \right) / c_1 \right) \tau} \tag{16}$$

A coordinate transformation is needed to make use of Eq. 10 to calculate the volume fluxes entering the (i,j) cell from the neighbor cells:

$$\xi_1^{(*)} = c_1 + \xi_1' \tag{17}$$

With this substitution, Eq. 14 becomes:

$$m_1^{(*)} \xi_1' + m_2^{(n)} \xi_2^{(n)} = \alpha' \tag{18}$$

where,

$$\alpha' = \alpha^{(*)} - m_1^{(*)} c_1 \tag{19}$$

To illustrate the method, the schematic sketch is shown in Fig. 2 (Zaleski *et al.*, 1999). The cell ABCD is assumed to be upwind of the cell ABHG. The segment ab is advected to cd. The flow also carries AB to EF. The volume gained by the downwind cell in the dark area.

3.2 Numerical Model

3.2.1 Staggered Grid for Navier-Stoke Equations

The staggered grid technology is used in order to avoid the unrealistic behavior of the discretized momentum equations for spatially oscillation pressures like the checkerboard pressure field. On a staggered grid the scalar variables (pressure, density, total enthalpy etc.) are stored at the nodes marked (•), whereas the velocities are located at the cell faces and are indicated by arrows. Horizontal (→) arrows

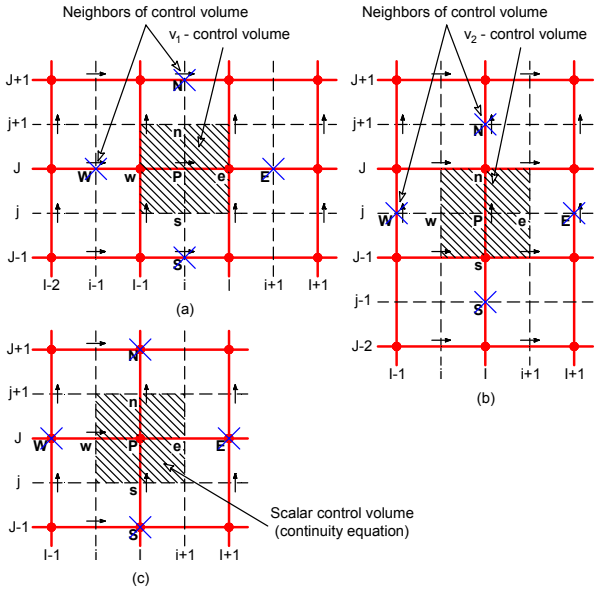

Fig. 3 The staggered grid for 2-D fluid flow

indicate the locations for v_1-velocities and vertical (↑) ones denote these for v_2-velocities.

3.2.2 Discretization of Momentum Equations

The fully implicit discretization of momentum equations can be expressed as:

$$a_P^{(v_i)} v_{i(P)} = \sum a_{nb}^{(v_i)} v_{i(nb)} + a_P^{0(v_i)} v_{i(P)}^0 + (p_{w(s)}^{(v_i)} - p_{e(n)}^{(v_i)}) A_P^{(v_i)} + b_P^{(v_i)} \tag{20}$$

Here $b_i^{(v_i)} = \overline{S} \Delta V^{(v_i)}$ are the momentum source terms; $A_P^{(v_i)}$ are the cell face areas of the v_i-control volumes; superscript 0 represents the previous time level. The neighbors involved in the summation $\sum a_{nb}^{(v_i)} v_{i(nb)}$ and prevailing velocities are shown in Figs. 3 (a and b).

The values of coefficients $a_P^{(v_i)}$ and $a_{nb}^{(v_i)}$ are calculated with the Hybrid differencing scheme suitable for convection-diffusion problem.

$$a_P^{(v_i)} = a_W^{(v_i)} + a_E^{(v_i)} + a_S^{(v_i)} + a_N^{(v_i)} + a_P^{0(v_i)} + \Delta F \tag{21}$$

$$a_P^{0(v_i)} = \frac{\rho_P^{0(v_i)} \Delta V^{(v_i)}}{\Delta t}$$

$$a_W^{(v_i)} = \max \left[\left(\rho v_1 A \right)_w^{(v_i)}, \left(\frac{\Gamma_w^{(v_i)}}{\delta x_{1(WP)}^{(v_i)}} A_w^{(v_i)} + \frac{\left(\rho v_1 A \right)_w^{(v_i)}}{2} \right), 0 \right]$$

$$a_E^{(v_i)} = \max \left[-\left(\rho v_1 A \right)_e^{(v_i)}, \left(\frac{\Gamma_e^{(v_i)}}{\delta x_{1(PE)}^{(v_i)}} A_e^{(v_i)} - \frac{\left(\rho v_1 A \right)_e^{(v_i)}}{2} \right), 0 \right]$$

$$a_S^{(v_i)} = \max\left[(\rho v_2 A)_s^{(v_i)}, \left(\frac{\Gamma_s^{(v_i)}}{\delta x_{2(SP)}^{(v_i)}} A_s^{(v_i)} + \frac{(\rho v_2 A)_s^{(v_i)}}{2} \right), 0 \right]$$

$$a_N^{(v_i)} = \max\left[-(\rho v_2 A)_n^{(v_i)}, \left(\frac{\Gamma_n^{(v_i)}}{\delta x_{2(PN)}^{(v_i)}} A_n^{(v_i)} - \frac{(\rho v_2 A)_n^{(v_i)}}{2} \right), 0 \right]$$

$$\Delta F = (\rho v_1 A)_e^{(v_i)} - (\rho v_1 A)_w^{(v_i)} + (\rho v_2 A)_n^{(v_i)} - (\rho v_2 A)_s^{(v_i)} \quad (22a\sim f)$$

The integrated form of continuity equation over a 2-D scalar control volume [see Fig. 3 (c)] becomes:

$$\frac{\rho_P - \rho_P^0}{\Delta t}\Delta V + \left[(\rho v_1 A)_e - (\rho v_1 A)_w \right] + \left[(\rho v_2 A)_n - (\rho v_2 A)_s \right] = 0 \quad (23)$$

The pressure correction equation is derived from the continuity equation, the equivalent of pressure correction equation for a 2-D transient flow will take the form:

$$a_P p'_P = a_W p'_W + a_E p'_E + a_S p'_S + a_N p'_N + b'_P \quad (24)$$

where $a_P = a_W + a_E + a_S + a_N$ and the coefficients are given below:

$$a_{W(E,S,N)} = (\rho dA)_{w(e,s,n)} \text{ with } d_{w(e,s,n)} = (A/a)_{w(e,s,n)}$$

$$b'_P = (\rho v_1^* A)_w - (\rho v_1^* A)_e + (\rho v_2^* A)_s - (\rho v_2^* A)_n + \frac{\rho_P^0 - \rho_P}{\Delta t}\Delta V \quad (25a\sim c)$$

where v_1^*, v_2^* are the guessed velocities.

The pressure correction equation is susceptible to divergence unless some under-relaxation is used during the iterative process.

3.2.3 Numerical Simulation Procedure

The flow chart of the numerical simulation is shown in Fig. 4. In this procedure, a coupling of PLIC-VOF method and SIMPLE algorithm is presented. In the VOF method, the volume fraction is propagated for the new time step based on the velocity from the previous time step and update phase averaged quantities. The SIMPLE algorithm is used to solve the flow field governing equations. In this algorithm, the convective fluxes per unit mass through cell faces are evaluated from so-called

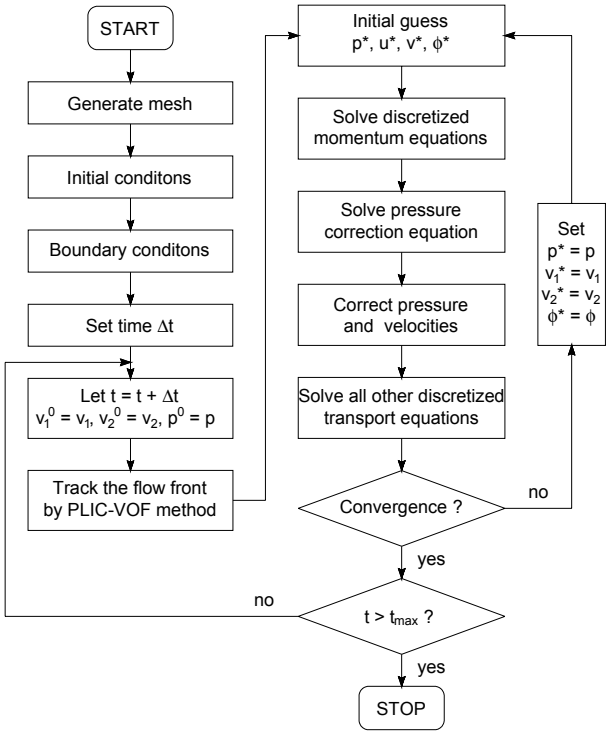

Fig. 4 Procedure of numerical simulation

guessed velocity components. Furthermore, a guessed pressure is used to solve the momentum equations, and a pressure correction equation, deduced from the continuity equation, is solved to obtain a pressure correction field, which is turn used to update the velocity and pressure fields. As the algorithm proceeds our aim must be progressively to improve these guessed fields. The process is iterated until convergence of the velocity and pressure field.

4. Numerical Results

The dam-breaking problem is considered as a good test to validate the precision of the free surface computation because of its simple initial and boundary conditions.

First example, two cases of dam-breaking with difference of the water columns corresponding to the experiment of Martin and Moyce (1952) are presented. The height and width of the water column of two cases are 2.25in×2.25in (5.715cm×5.715cm) and 2.25in×4.5in (5.715cm×11.43cm), respectively. A uniform Cartesian grid system with grid size (0.025×0.025) employed on the dimensionless domain is used.

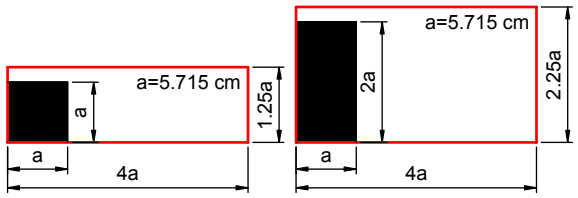

Fig. 5 Dimensions and initial conditions for two test cases

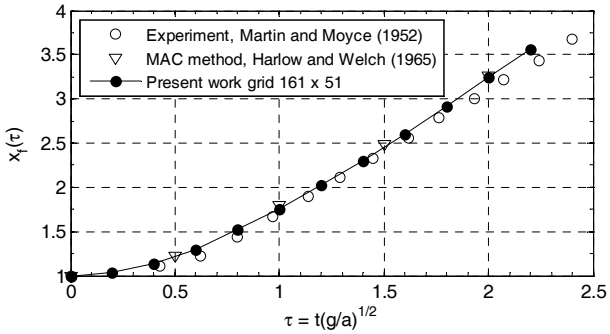

Fig. 6 A comparison of the waterfront from present result, experimental data, and other numerical result for the case of 5.715cm×5.715cm

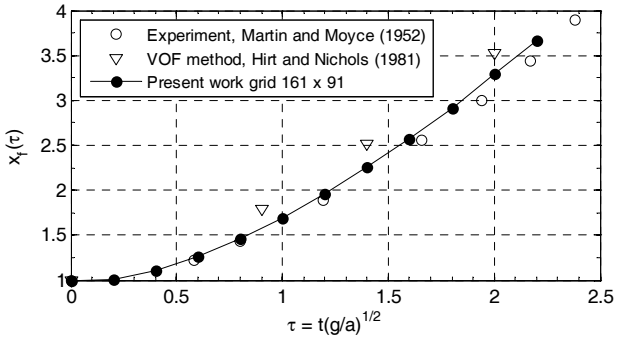

Fig. 7 A comparison of the waterfront from present result, experimental data, and other numerical result for the case of 5.715cm×11.43cm

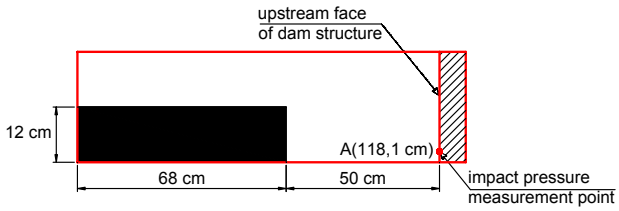

Fig. 8 A schematic of the dam-breaking simulation corresponding to the experiment by Hu and Kashiwagi(2004)

Figs. 6 and 7 show the waterfront position at different times from the numerical results. The available experimental data of Martin and Moyce (1952) and other existing numerical results: MAC method developed by Harlow and Welch (1965), SLIC-VOF method developed by Hirt and Nichols (1981) are also plotted in these figures. It can be seen that the present works show much better agreement with experiment.

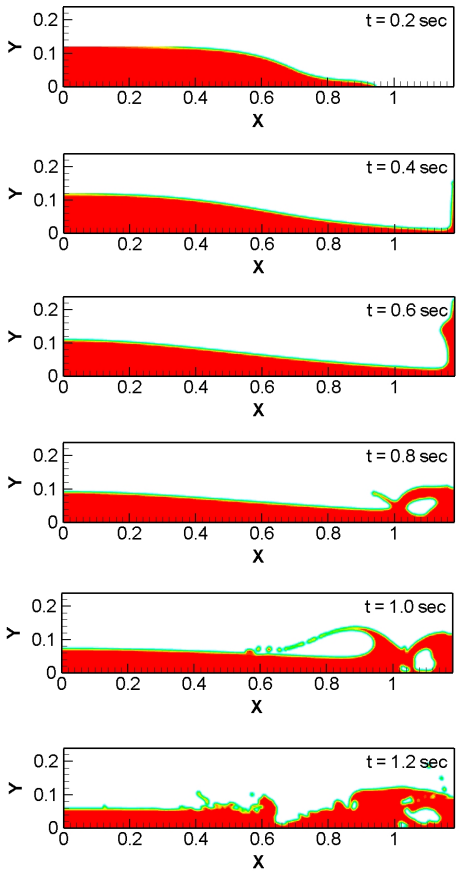

Fig. 9 Dam-breaking flow and impact against the downstream wall of tank at time t=0.2, 0.4, 0.6, 0.8, 1.0, 1.2sec

Second example, the water impact pressure on a vertical wall is numerically measured and compared with experimental data and previous study. A schematic of the dam-breaking model is presented in Fig. 8. In this model, the tank size is 118cm×24cm and a column of water (68cm×12cm) is located in the left side of tank. For impact pressure measurement, similar to the experiment of Hu and Kashiwaki (2004), a point A (118,1cm) is defined on the downstream wall of tank.

Fig. 9 shows some snapshots of water flow at different times. After the water column is allowed to flow, a relatively high velocity and shallow water depth flow in the x-direction quickly forms (t=0~0.32 sec). As time progresses, the flow impacts on the

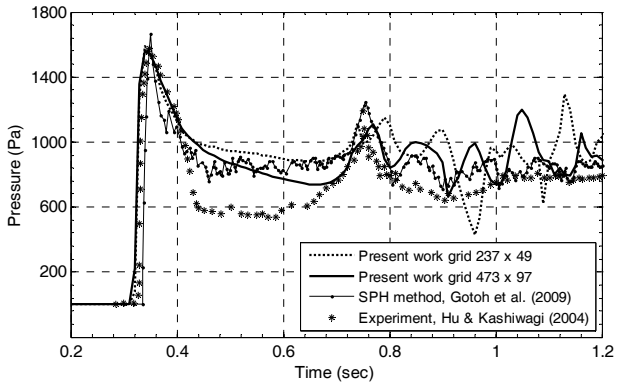

Fig. 10 Time variation of the impact pressure at point A using two types of grid compared with experimental data and other numerical result

vertical wall at the opposite side of tank, and reaches highest pressure at t=0.34sec. An upward water jet is suddenly formed that rises until gravity overcomes the upward momentum (around t=0.52sec). At this moment, the jet becomes thicker and the flow starts to reverse. For t 〉 1.2sec, the overall momentum of the flow has reduced considerably, therefore, analysis of the flow beyond this point is of no practical significance.

To perform a grid refinement test, two types of grid: 237×49 and 473×97 grid points are used. Fig. 10 shows a comparison of the time series of the impact pressure at point A, for which the computations are performed using two different grids.

As shown in the figure, the values of water impact pressure on the wall are pretty much the same in all two girds until the water has returned from the wall (after 0.32sec) and the highest pressures are almost the same with experimental data. After that some differences occur, the coarse grid is clearly not good enough. For computation with finer grid (473×97), the position of first peak and its values agree well with the experimental data and other numerical result developed by Gotoh *et al.* (2009).

5. Conclusions

In this paper, a new algorithm for incompressible free surface flows has been introduced to simulate the water impact pressure load acting on the upstream face of a dam structure. A set of equations has been used to represent the motion of fluid flows, and the governing equations are solved numerically on a uniform staggered Cartesian grid by coupling of FVM with the full-implicit scheme and explicit geometric PLIC-VOF method.

Numerical examples of three dam-breaking problems are computed to predict the waterfront position and water impact pressure on the vertical wall. The results of the dam-breaking simulation are in good agreement with the experimental data. The general behaviour of the fluid is the same and the impact peak of the pressure on the wall have been precisely simulated. It can be concluded that the present algorithm is robust and efficient to be used for computation of flood impact pressure acting on a upstream face of dam and similar structures.

References

Aulisa, E., Manservisi, S., Scardovelli, R., Zaleski, S. (2007) Interface Reconstruction with Least-Square Fit and Split Advection in Three-Dimensional Cartesian Geometry, *J. Comput. Phys.*, 255(2), pp.2301~2319.

Brackbill, J.U., Kothe, D.B., Zemach, C. (1992) A Continuum Method for Modeling Surface Tension, *J. Comput. Phys.*, 100(2), pp.335~354.

Gueyffier, D., Nadim, A., Li, J., Scardovelli, R., Zaleski, S. (1999) Volume of Fluid Interface Tracking with Smoothed Surface Stress Methods for Three-dimensional Flows, *J. Comput. Phys.*, 152, pp.423~456.

Harlow, F.H., Welch, J.E. (1965) Numerical Calculation of Time-Dependent Viscous Incompressible Flow of Fluid with Free Surface, *Phys. Fluids*, 8, pp.2182~2188.

Hirt, C.W., Nichols, B.D. (1981) Volume of Fluid (VOF) Method for the Dynamics of Free Boundaries, *J. Comput. Phys.*, 39, pp.201~225.

Hu, C., Kashiwagi, M. (2004) A CIP-based Method for Numerical Simulation of Violent Free-surface Flows, *J. Mar. Sci. Technol.*, 9, pp.143~157.

Khayyer, A., Gotoh, H., Shao, S.D. (2009) Enhanced Predictions of Wave Impact Pressure by Improved

Incompressible SPH Methods, *Applied Ocean Research,* 31(2), pp.111~131.

Kleefsman, K.M.T, Fekken, G., Veldman, A.E.P, Iwanowski, B., Buchner, B. (2005) A Volume-of-Fluid Based Simulation Method for Wave Impact Problems, *J. Comput. Phys.,* 206, pp.363~393.

Li, J. (1995) Calcul d'interface Affine par Morceaux (Piecewise Linear Interface Calculation), *C. R. Acad. Sci. Paris, série IIb,* Paris, 320, pp.391~396.

Martin, J.C., Moyce, W.J. (1952) An Experimental Study of the Collapse of Liquid Columns on a Rigid Horizontal Plane, *Philos. Trans. R. Soc.,* A244, pp.312~324.

Noh, W.F., Woodward, P. (1976) SLIC(Simple Line Interface Calculation), *Proceeding of the fifth International Conference on Numerical Methods in Fluid Dynamics,* 59, pp.330~340.

Parker, B.J., Youngs, D.L. (1992) Two and Three Dimensional Eulerian Simulation of Fluid Flow with Material Interfaces, *Technical Report,* 01/92.

Patankar, S.V., Spalding, D.B. (1972) A Calculation Procedure for Hear, Mass and Momentum Transfer in Three-Dimensional Parabolic Flows, *Int. J. Heat Mass Transfer,* 15(10), pp.1787~1806.

Rider, W.J., Kothe, B.D. (1998) Reconstruction Volume Tracking, *J. Comput. Phys.,* 141, pp.112~152.

Scardovelli, R., Zaleski, S. (2003) Interface Reconstruction with Least-Square Fit and Split Eulerian-Lagrangian Advection, *Int. J. Numer. Meth. Fluids*, 41, pp.251~274.

Wei, Y., Shu-hong, L., Yu-lin, W. (2010) An Unsplit Lagrangian Advection Schtie for Volume of Fluid Method, *Journal of Hydrodynamics,* 22(1), pp.73~80.

Youngs, D.L. (1986) Time-dependent Multi-Material Flow with Large Fluid Distribution, *Numerical Method for Fluid Dynamics,* pp.187~221.

● 논문접수일 2010년 10월 30일
● 논문심사일 2010년 11월 4일
● 게재확정일 2010년 12월 6일